

Review

# Looking for Signatures of AGN Feedback in Radio-Quiet AGN

Preeti Kharb <sup>\*,†</sup>  and Sasikumar Silpa <sup>†</sup> 

National Centre for Radio Astrophysics, Tata Institute for Fundamental Research (NCRA-TIFR),  
Savitribai Phule Pune University, Ganeshkhind, Pune 411007, India

\* Correspondence: kharb@ncra.tifr.res.in

† These authors contributed equally to this work.

**Abstract:** In this article, we discuss the state of “AGN feedback” in radio-quiet (RQ) AGN. This study involves heterogeneous samples of nearby Seyfert and LINER galaxies as well as quasi-stellar objects (QSOs) that have been observed at low radio frequencies (few  $\sim 100$  MHz) with the upgraded Giant Meterwave Radio Telescope (GMRT) and  $\sim$ GHz frequencies with the Karl G. Jansky Very Large Array (VLA) and Very Long Baseline Array (VLBA). These multi-frequency, multi-resolution observations detect a range of arcsecond-scale radio spectral indices that are consistent with the presence of multiple contributors including starburst winds and AGN jets or winds; steep spectrum “relic” emission is observed as well. Polarization-sensitive data from the VLA and GMRT suggest that the radio outflows are stratified (e.g., in IIZw2, Mrk231); distinct polarization signatures suggest that there could either be a “spine + sheath” structure in the radio outflow, or there could be a “jet + wind” structure. Similar nested biconical outflows can also explain the VLBA and SDSS emission-line data in the KISSR sample of double-peaked emission-line Seyfert and LINER galaxies. Furthermore, the modeling of the emission-lines with plasma modeling codes such as MAPPINGS indicates that parsec-scale jets and winds in these sources can disturb or move the narrow-line region (NLR) gas clouds via the “shock + precursor” mechanism. Apart from the presence of “relic” emission, several Seyfert and LINER galaxies show clear morphological signatures of episodic jet activity. In one such source, NGC2639, at least four distinct episodes of jets are observed, the largest one of which was only detectable at 735 MHz with the GMRT. Additionally, a  $\sim 6$  kpc hole in the CO molecular gas along with a dearth of young stars in the center of its host galaxy is observed. Multiple jet episodes on the 10–100 parsec scales and a  $\sim 10$  parsec hole in the molecular gas is also observed in the Seyfert galaxy NGC4051. This suggests a link between episodic jet activity in RQ AGN and “AGN feedback” influencing the evolution of their host galaxies. However, a similar simple relationship between radio outflows and molecular gas mass is not observed in the Palomar–Green (PG) QSO sample, indicating that “AGN feedback” is a complex phenomenon in RQ AGN. “AGN feedback” must occur through the local impact of recurring multi-component outflows in RQ AGN. However, global feedback signatures on their host galaxy properties are not always readily evident.

**Keywords:** quasars; Seyfert galaxies; LINER galaxies; radio continuum emission; polarimetry; very long baseline interferometry

## 1. Introduction

Galaxy evolution is one of the leading open questions in astrophysics (e.g., [1]). The observational findings of a close link between the galaxy properties, such as bulge mass and stellar velocity dispersion, and its central supermassive black hole (SMBH) have led astronomers to believe that the SMBH with its parsec-scale sphere of influence can affect the kpc-scale galaxy bulge through the process of “Active Galactic Nuclei (AGN) feedback” [2,3]. AGN are believed to regulate galaxy growth by injecting energy into the surrounding gas, which has the effect of

arXiv:2302.06954v1 [astro-ph.GA] 14 Feb 2023



**Citation:** Kharb, P.; Silpa, S. Looking for Signatures of AGN Feedback in Radio-Quiet AGN. *Galaxies* **2023**, *11*, 27. <https://doi.org/10.3390/galaxies11010027>

Academic Editors: Stefi Baum and Christopher P. O’Dea

Received: 15 December 2022

Revised: 21 January 2023

Accepted: 2 February 2023

Published: 8 February 2023



**Copyright:** © 2023 by the authors. Licensee MDPI, Basel, Switzerland. This article is an open access article distributed under the terms and conditions of the Creative Commons Attribution (CC BY) license (<https://creativecommons.org/licenses/by/4.0/>).

either heating and/or expelling star-forming gas (“negative feedback”) or facilitating localized star-formation (“positive feedback”) [2,4–6]. “AGN feedback” can occur through radiative power (“quasar mode”, e.g., [7,8]) or mechanical power fed back into the galaxy through AGN winds and jets (“maintenance/jet mode”, e.g., [5,9–11]). The observational and energetic signatures of this “AGN feedback” are, however, still far from being unambiguous [3,12]. While highly collimated jets cannot be efficient agents of “AGN feedback”, presumably due to the smaller working surfaces at their advancing ends, relatively isotropic impacts via changes in jet direction can be highly effective, as can broader AGN outflows and winds [3].

Radio-quiet (RQ) AGN that comprise greater than 80% of the AGN population, however, have small-scale jets on the parsec to hundreds of parsec scales [13–16], but typically not extending beyond  $\sim 10$  kpc [17,18]; their total radio luminosities do not overwhelm their optical luminosities [19]. Recent work using 6 GHz Very Large Array (VLA) data of SDSS quasi-stellar objects (QSOs) by Kellermann et al. [20] has suggested that RQ AGN have  $21 \leq \log[L_6(\text{W Hz}^{-1})] \leq 23$ . RQ AGN also tend to be low luminosity AGN (LLAGN) and comprise Seyfert nuclei and LINER galaxies [21,22]. Ho [23] have identified LLAGN as those with  $\text{H}\alpha$  line luminosities ranging from  $10^{37}$  to  $10^{41}$  erg  $\text{s}^{-1}$  or with bolometric luminosities in the range  $L_{\text{bol}} \lesssim 10^{37} - 10^{44}$  erg  $\text{s}^{-1}$  and Eddington ratios in the range  $L_{\text{bol}}/L_{\text{Edd}} \sim 10^{-9} - 10^{-1}$  [24]. In this article, we use LLAGN and RQ AGN interchangeably when referring to Seyferts, LINERs, and RQ quasars (which we use in lieu of QSOs).

Jet–interstellar medium (ISM) interaction has been inferred or observed in several RQ AGN in the literature. For example, in IC5063, NGC5643, NGC1068, and NGC1386 (as part of the Measuring Active Galactic Nuclei Under MUSE Microscope (MAGNUM) Survey; [25]), IC5063 [5,26,27], NGC1266 [28], HE 0040-1105 from the Close AGN Reference Survey (CARS) survey [29], and subset of sources from the Quasar Feedback Survey [30–33]. Evidence for an interaction between the AGN-driven winds and ISM has also been reported for RQ AGN in the literature (e.g., [34–39]). Therefore, despite the lack of large and powerful radio outflows in RQ AGN, they can be effective agents for AGN feedback.

In this review, we discuss the radio observations at multiple spatial resolutions of samples of Seyferts, LINERs, and RQ quasars. We review the results from multi-frequency as well as multi-scale observations going from arcsecond scales with the upgraded Giant Meterwave Radio Telescope (GMRT) and the Karl G. Jansky Very Large Array (VLA) in Sections 2–4, to milli-arcsec scales with the Very Long Baseline Array (VLBA), of nearby low luminosity or radio-quiet AGN in Section 5, and we discuss the state of “AGN feedback” in them. All sources lie at redshifts  $< 0.1$ , which correspond to spatial scales smaller than  $\sim 2$  parsec on milli-arcsec and  $\sim 2$  kpc on arcsec scales. We assume a cosmology with  $H_0 = 73$  km  $\text{s}^{-1}$   $\text{Mpc}^{-1}$ ,  $\Omega_{\text{mat}} = 0.27$ ,  $\Omega_{\text{vac}} = 0.73$ . Spectral index  $\alpha$  is defined such that the flux density at frequency  $\nu$  is  $S_\nu \propto \nu^\alpha$ .

## 2. Low Radio Frequency Observations of RQ AGN

Low-frequency radio (few  $\sim 100$  MHz) observations with the GMRT have typically detected radio emissions from both the AGN as well as stellar-related activity from the host galaxies of Seyferts or LINERs (e.g., [18,40–42]). In these data, radio emission from the Seyferts/LINERs is lobe-like or bubble-like but often simply in the form of extended diffuse emission without distinct morphological features. The radio spectral index images cannot distinguish between the AGN and stellar-related emission either. While the stellar-related emission is typically steep ( $\alpha \leq -0.7$ ), the AGN emission even in the unresolved “cores” can be either flat ( $\alpha \geq -0.5$ ) or steep. Steep spectrum “cores” are likely to be due to the large beam of the GMRT including optically thin jet or lobe emission on sub-arcsec scales. The presence of additional lobes on arcsec scales has been indicated in the GMRT 325 and 610 MHz observations of the Seyfert galaxies, NGC3516, NGC5506, NGC5548, NGC5695 (Rubinur et al. in prep.).

GMRT observations can probe additional activity episodes as large steep-spectrum diffuse lobes/bubbles or as “relic” lobe emission that is no longer being supplied with particles and fields from the AGN (e.g., [40,43–45]). The lobes of the Seyfert galaxy NGC4235 with abruptly changing spectral indices between two sets of lobes represent one such case (see Figure 1; [40]). Both the 610 MHz image and the 325–610 MHz spectral index image of NGC4235 hinted at diffuse steep-spectrum radio emission just beyond the well-defined western lobe and enveloping it. While the average spectral index is  $-0.29 \pm 0.19$  in the western lobe and  $-0.56 \pm 0.24$  in the eastern lobe, the average spectral index is  $-1.82 \pm 0.17$  in this extended region. The average spectral index errors come from a spectral index noise image. The robustness of the steep spectrum emission is discussed in greater detail by Kharb et al. [40]. This surrounding steep-spectrum emission is reminiscent of “relic” radio emission, as observed in the lobes of the radio galaxy 3C388 by Roettiger et al. [46], where a lobe with an average spectral index of  $\sim -0.8$  was surrounded by the steep-spectrum emission of spectral index  $\sim -1.5$  from a previous AGN activity episode. Based on a simple spectral aging analysis in NGC4235, the relic outer lobe appeared to be at least two times older than the present lobe. This implied that the AGN in NGC4235 was switched “off” for the same time that it has been “on” for the current episode [40].

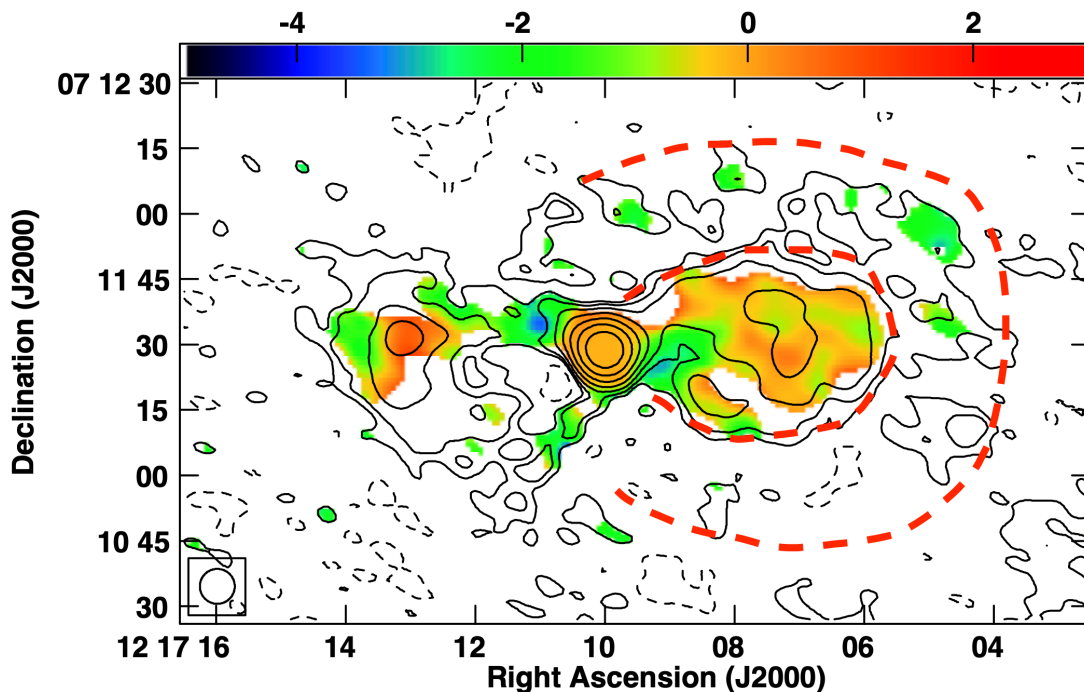


**Figure 1.** The 325–610 MHz spectral index image from the GMRT in color overlaid with the 610 MHz radio contours for the Seyfert galaxy NGC4235. The average spectral index is  $\sim -0.6$  in the lobes and  $\leq -1.8$  in the “relic” lobe (emission between the red dotted lines). The contour levels are in percentage of the peak intensity and increase by factors of two. The peak intensity and lowest contour levels are  $2.3 \times 10^{-2} \text{ Jy beam}^{-1}$  and  $\pm 0.3\%$  of the peak intensity, respectively. The contour image is convolved with a circular beam of size 8 arcsec. Image reproduced from Kharb et al. [40].

### 3. Jet Driven Feedback: The Case of NGC2639

Sanders [47] had predicted that Seyfert activity must be episodic on timescales of  $10^4$ – $10^5$  years during its statistical lifetime of  $3$ – $7 \times 10^8$  years. They had arrived at these numbers based on the typical extent of the radio outflows as well as the NLR in Seyfert galaxies. A Seyfert galaxy must therefore undergo  $\sim 100$  activity episodes during its lifetime. Clear examples

of episodic jet activity in Seyfert and LINER galaxies have been identified in only a couple of sources, viz., Mrk6 [48], NGC2992 [49], and NGC2639 [50]. Sebastian et al. [51] had found tentative signatures for multiple jet episodes in a majority (~55%) of their small Seyfert galaxy sample of nine sources. This fraction appeared to be higher than that has been reported in radio-loud (RL) AGN (~10–15% in radio galaxies [52]) (see also the 3D GRMHD jet simulations of Lalakos et al. [53] that reproduce these low fractions). However, signatures of ~100 episodes are almost never observed in Seyferts or LINERs, at least in the radio outflows. This might not be due to their true absence but rather due to the difficulty in their identification due to the low surface brightness of Seyfert/LINER lobes, their small spatial extents, lack of collimated jets, and confusion with the radio emission from stellar-related activity (star-formation, supernovae, and starburst winds) arising in the host galaxy.

Sebastian et al. [50] had noted the presence of at least three episodes in NGC2639 with two sets of bipolar radio lobes detected with the VLA and oriented nearly perpendicular to each other, similar to what was observed in Mrk6, as well as a parsec-scale core–jet structure detected with the Very Long Baseline Array (VLBA) and oriented at least 30 degrees from the sub-kpc east–west oriented radio lobes. GMRT observations at 325 and 735 MHz showed the presence of an additional pair of radio lobes, oriented nearly 45 degrees from the previously known north–south lobes (see Figure 2; [45]). It is worth pointing out that there is no continuous connecting radio emission between different jet episodes. Rather, the jets and lobes in each episode have clearly defined hotspots or edges distinguishing them as independent events, making a single precessing jet model fitting all of the radio emission improbable.

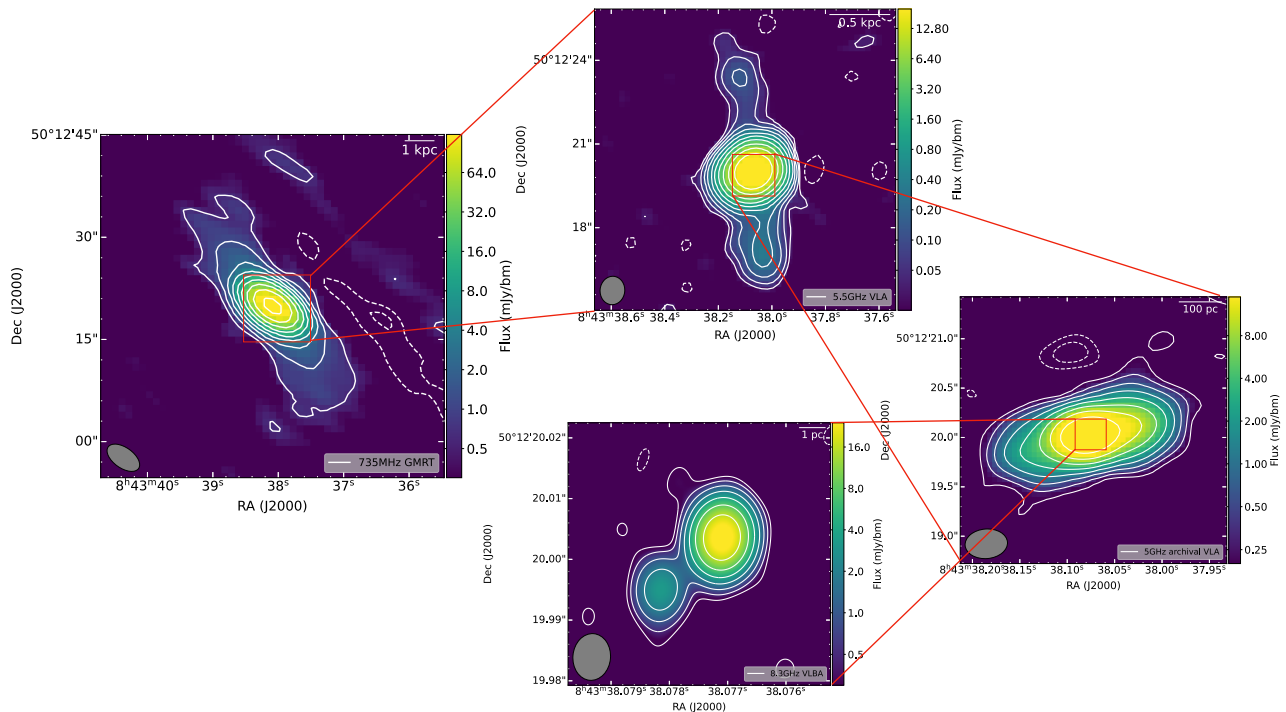


**Figure 2.** The four AGN jet episodes of NGC2639. (Left) 735 MHz GMRT total intensity image. The  $\sim 9$  kpc radio lobes are seen in this image. Contour levels:  $(-2, -1, 1, 2, 4, 8, 16, 32, 64, 128, 256) \times 0.6$  mJy beam $^{-1}$ . The beam at the bottom left corner is of size: 5.48 arcsec  $\times$  3.0 arcsec at PA = 54.6 degrees. (Top) 5.5 GHz VLA total intensity image. Contour levels:  $(-2, -1, 1, 2, 4, 8, 16, 32, 64, 128, 256, 512) \times 0.03$  mJy beam $^{-1}$ . The  $\sim 1.5$  kpc north-south radio jets are seen here. Beam size: 1.02 arcsec  $\times$  0.89 arcsec at PA =  $-5.8$  degrees. (Right) 5 GHz VLA radio image. Contour levels:  $(-2, -1, 1, 2, 4, 8, 16, 32, 64, 128) \times 0.164$  mJy beam $^{-1}$ . The  $\sim 360$  parsec east-west lobes are seen in this image. Beam size: 0.43 arcsec  $\times$  0.30 arcsec at PA =  $-85.4$  degrees. (Bottom) 8.3 GHz VLBA image showing a  $\sim 3$  parsec jet at PA = 130 degrees. Contour levels:  $(-2, -1, 1, 2, 4, 8, 16, 32, 64) \times 0.239$  mJy beam $^{-1}$ . Beam size: 7.7 mas  $\times$  6.2 mas at PA =  $-4.9$  degrees. Figure reproduced from Rao et al. [45]. A  $\sim 6$  kpc hole in the molecular gas distribution is observed in the central regions of NGC2639.

Ages of the three pairs of lobes were derived using the spectral aging software BRATS, which stands for Broadband Radio Astronomy Tools [54], and they turned out to be, respectively,  $34_{-6}^{+4}$  million years,  $11.8_{-1.4}^{+1.7}$  million years, and  $2.8_{-0.5}^{+0.7}$  million years, with the GMRT lobes being the “on” and “off” times of these jets or lobes (using the spectral age of a given set of lobes and the spectral age difference between two sets of lobes, respectively), the AGN jet duty cycle in NGC2639 turns out to be  $\sim 60\%$ . Based on the molecular gas data from the EDGE [55]—Calar Alto Legacy Integral Field Area (CALIFA [56]) survey, Ellison et al. [57] have found that the gas fraction in the central region of NGC2639 is a factor of a few lower than in star-forming regions, suggesting that the AGN has partially depleted the central molecular gas reservoir. Like the CO (1-0) molecular gas image, which shows a hole with a diameter of  $\sim 6$  kpc, the GALEX NUV image also shows a deficiency of star formation in the last 200 million years in the inner  $\sim 6$  kpc region of NGC2639. These results point to star-formation quenching taking place in the central regions of NGC2639.

If the CO (1-0) molecular gas ring is a result of push-back from the jet in NGC2639, the  $PV$  (pressure times volume) amount of work done on the molecular gas by the jet to create a cavity can be estimated. Rao et al. [45] have shown that for the CO gas ring radius of 3 kpc, the volume

of the disk-like cavity is  $1.25 \times 10^{66} \text{ cm}^3$ , and the  $PV$  work done is  $>3.44 \times 10^{54} \text{ erg}$ . Using the lobe flux densities at 5 GHz, the time-averaged power (e.g., using the relations in [58]) for a spectral age of 2.8 million years is  $6.8 \times 10^{56} \text{ erg}$ . Therefore, only  $\sim 0.5\%$  of the east–west jet power is sufficient to push back the CO gas in NGC2639. Similarly small fractions are needed from the north–south jets and the north–east–south–west jets. However, the creation of a hole in the molecular gas in the galactic center likely required several jet episodes to occur, given that each jet episode is collimated and therefore highly directional [45].

NGC2639 or Mrk6 are not unique in showing signatures of radio jets or lobes that have different sky orientations when looked at with multiple spatial resolutions. Another case is the famous Seyfert galaxy, NGC4051. Multi-resolution images of NGC4051 from Jones et al. [59] and Giroletti and Panessa [60] show at least three sets of radio lobes or jets. At a resolution of  $\sim 2 \text{ arcsec}$ , there lies a double-lobed radio structure of extent  $\sim 830 \text{ parsec}$  at a PA of 30 degrees (at its redshift of 0.002336, 1 arcsec corresponds to 61 parsecs). At a resolution of  $\sim 0.5 \text{ arcsec}$ , there is a jet–core–jet structure of extent  $\sim 90 \text{ parsec}$  at a PA of 60 degrees. Finally, on the 100 mas scale as probed by the European VLBI Network (EVN), the parsec-scale core–jet structure shows a faint extension toward the south (See Figure 3). Interestingly, NGC4051 also appears to have a hole with a diameter of  $\sim 10 \text{ parsecs}$  in its molecular gas distribution, as observed from Gemini North (data from Riffel et al. [61] reanalyzed by D. May et al. <sup>1</sup>). Overall, NGC2639 and NGC4051 could be candidates for the presence of jet-driven “negative AGN feedback” in RQ AGN.

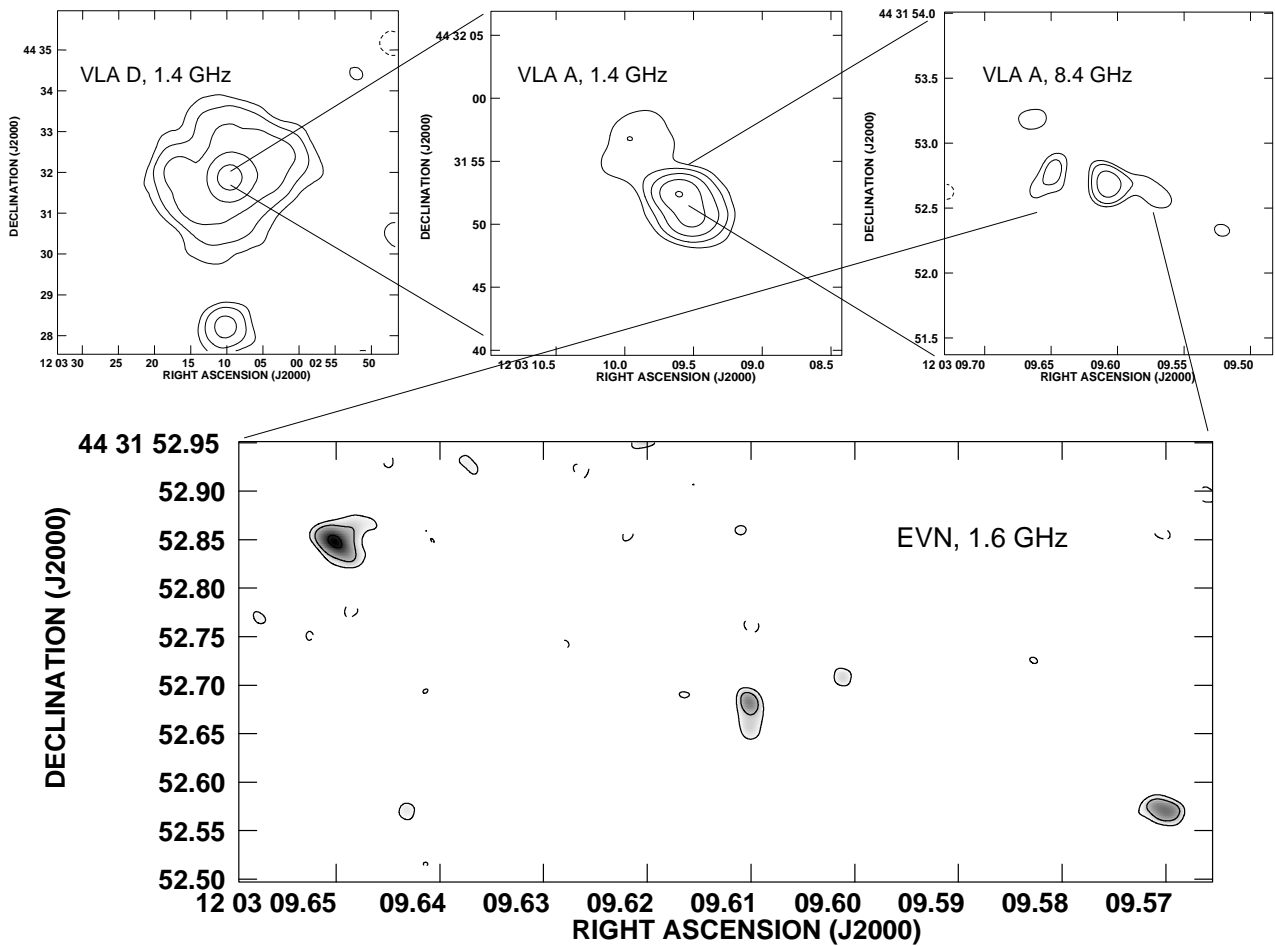


**Figure 3.** The three radio lobes or jets at different position angles in the Seyfert galaxy NGC4051. The leftmost panel (VLA 1.4 GHz) image shows the galactic emission surrounding the 1 kpc-sized radio AGN. The middle panel shows  $\sim 830$  parsec lobes at a PA of 30 degrees. The rightmost panel shows a  $\sim 90$  parsec lobes at a PA of 60 degrees. The bottom panel shows the EVN image with a parsec-scale core–jet structure, showing a faint extension toward the south. Figure reproduced from Giroletti and Panessa [60]. A  $\sim 10$  parsec hole in the molecular gas distribution is observed in the central regions of NGC4051.

#### 4. Jet + Wind Driven Feedback

##### 4.1. The Palomar–Green Radio-Quiet Quasar Study on Kpc-Scales

We now discuss the case of the Palomar–Green (PG; [62]) sample of RQ quasars, which has extensive multi-resolution radio jet and multi-phase gas outflow data, in the literature. Silpa et al. [43] carried out a 685 MHz GMRT study of the PG RQ quasar sample and found that the two-frequency radio spectral indices (using the GMRT and VLA) were ultra-steep ( $\alpha \leq -1.0$ ) in few of the sources. Other than a correlation between the total GMRT 685 MHz luminosity and Eddington ratios, other radio properties of the sample such as radio core sizes and radio spectral indices did not correlate with BH properties such as their masses or Eddington ratios. This suggested either that the radio emission was stellar-related or was due to previous jet episodes (i.e., “relic” emission) in them (see Section 3). A combined GMRT–VLA study of the PG RQ sample has shown evidence for the presence of small-scale, bent, and low-powered jets in a couple of sources (see Section 5 ahead), while for the rest, it was difficult to unambiguously

determine the origin of radio emission (whether via jet or wind or stellar processes; [63]). Multi-frequency, multi-resolution radio polarization observations have detected a stratified radio outflow in PG 0007+106 (a.k.a. III Zw 2 [44]). The stratified radio outflow could either be a “spine + sheath” structure in the jet or a “jet + wind” composite structure (see Figure 4). Each component of the stratified outflow is observed to have a characteristic magnetic (B) field geometry (e.g., [64,65]). B fields are aligned with the jet direction in the case of a jet or jet “spine” while they are transverse in the case of a wind or jet “sheath”. The parallel B fields could represent the poloidal component of a large-scale helical B field, while the transverse B fields could either represent the toroidal component of the helical field or a series of transverse shocks that order B fields by compression. Alternately, they could represent toroidal B fields threading an AGN wind or jet “sheath”, which is sampled in the lower-resolution images. The bow-shock-like feature at the termination point of the VLA jet (see Figure 5 of [44]), and the presence of a misaligned “sputtering” lobe in the GMRT image (annotated as ML in Figure 4), are consistent with restarted jet activity in III Zw 2.

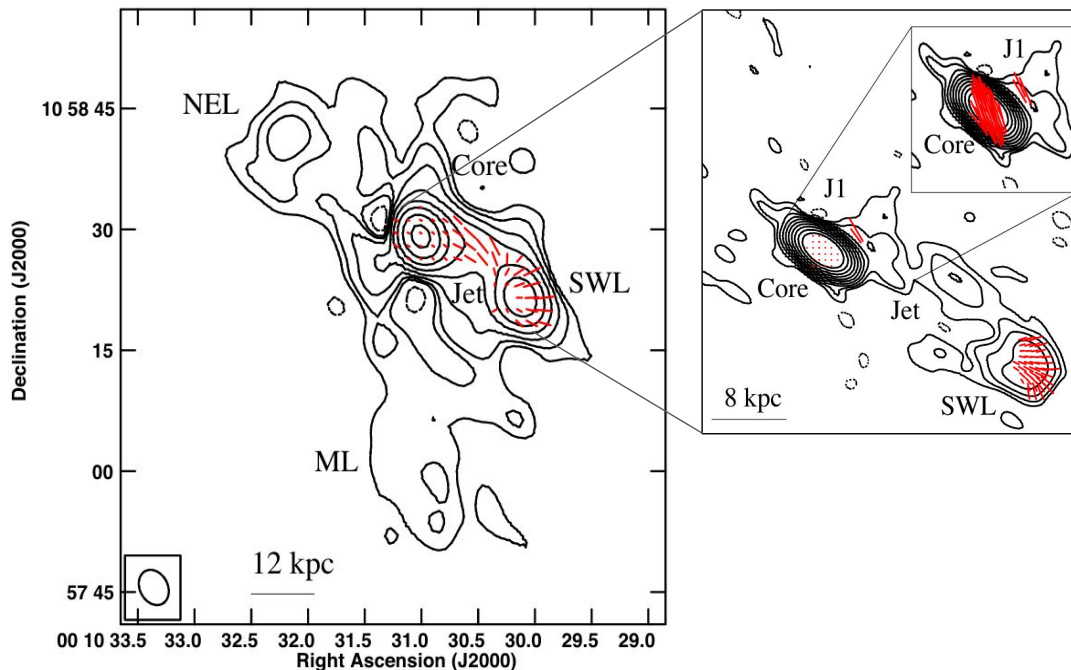


**Figure 4.** The GMRT 685 MHz total intensity contour image of III Zw 2 superimposed with red fractional polarization vectors, with 2 arcsec length of the vector corresponding to 6.25% fractional polarization. The inset on the right presents the VLA 5 GHz total intensity contour image of the south-western jet-lobe region, superimposed with red fractional polarization vectors, with 1 arcsec length of the vector corresponding to 25% fractional polarization. The smallest inset on the top right presents the VLA 5 GHz total intensity contour image of the radio core with red polarized intensity vectors, with 1 arcsec length of the vector corresponding to 0.031 mJy beam<sup>-1</sup> polarized intensity. The peak contour surface brightness is  $x$  mJy beam<sup>-1</sup> and the levels are  $y \times (-1, 1, 2, 4, 8, 16, 32, 64, 128, 256, 512)$  mJy beam<sup>-1</sup>, where  $(x ; y)$  are (35, 0.21) and (124, 0.05) for the GMRT and VLA images respectively. Figure reproduced from Silpa et al. [44].

The 5 GHz jet kinetic power of a subset of the PG RQ quasars estimated using the empirical relation of Merloni and Heinz [58] is within the range  $10^{42}$ – $10^{43}$  erg s<sup>-1</sup> [63]. For these jet powers, either stellar-mass loading (e.g., [66,67]) or the growth of Kelvin–Helmholtz (KH) instabilities triggered by recollimation shocks/jet–medium interactions can effectively decelerate

and decollimate the jets (e.g., [68,69]). As the jets propagate through the host galaxy, they would encounter numerous stars, which inject matter into the jets via stellar winds. The mixing of the injected stellar material with the jet plasma causes the jets to decelerate. Using a small sample of RQ quasars, Silpa et al. [32] found that the polarized radio emission and [O III] emission did not always spatially overlap. This was suggested to arise from the depolarization of radio emission by either an irregular Faraday screen of clumpy emission-line gas or by the emission-line gas that had entrained and mixed with the synchrotron plasma in the lobes. While modeling the former scenario, the fluctuation scales of the electron density (or, equivalently the sizes of the emission-line gas clumps or clouds, or filaments) were considered and estimated. This value was also assumed to represent the fluctuation scales of the random B-field component while modeling the latter scenario. Interestingly, the lower limit on the size value ( $\sim 10^{-5}$  parsec) matches the sizes of red giant stars. KH instabilities also promote entrainment and mixing between the surrounding gas and the jet plasma, resulting in the deceleration and decollimation of the jets. KH instabilities can also cause jet bending (e.g., [70,71]). Signatures of KH instabilities include knotty polarization structures and the presence of poloidal magnetic fields (e.g., [72]). Both of these signatures are observed in the few RQ quasars that are detected in polarized light. *Overall, therefore, there is evidence for small (arcsec) scale jet–medium interaction taking place in these sources.*

Shangguan et al. [73] have found that the molecular gas masses and kinematics of the PG quasars were similar to those of the star-forming galaxies. Additionally, no molecular gas outflows were detected in these sources. Their host galaxies were found to be following the “Kennicutt–Schmidt law” [74], suggesting that no star formation quenching was taking place in them. In the recent work of Molina et al. [75], the molecular gas kinematics of the PG quasar host galaxies also suggest that the “negative AGN feedback” is ineffective in them. In general, there appears to be no immediate significant impact on the global molecular gas reservoirs by jets or outflows in the PG sources. However, the possibility that the AGN might be impacting the ISM locally cannot be ruled out (e.g., [76]). As discussed above, we infer the presence of localized jet–medium interaction from the jet kinetic power argument as well as the polarization data in the PG RQ quasar sample. Localized impact on the gas by AGN or jets could in principle be captured by spatially resolved observations of multiple and higher CO transitions (e.g., [77–87]).

One of the plausible mechanisms for star-formation quenching as proposed in the literature includes galaxy major and minor mergers (along with “AGN feedback” in most cases [88–95]). The galaxy major merger simulations by Springel et al. [96] show that the presence of accreting BHs can significantly impact the merger dynamics. Galaxy mergers can also cause enhanced star-forming activity [97–99] just as a “positive AGN feedback” process [100,101]. On the other hand, Weigel et al. [102] suggest that the major merger quenching cannot fully explain the slow evolution of galaxies from blue to red; alternative quenching mechanisms (“AGN feedback” being a potential candidate) are needed. The host galaxies of a large fraction of the PG RQ quasars show signatures of ongoing galactic mergers [43]. Therefore, the merger scenario can also have an influence on the overall interpretation of AGN feedback.

#### 4.2. The Jet and Wind in Mrk231

We now discuss the case of the quintessential AGN that clearly hosts both a jet and wind component and is routinely considered in “AGN feedback” scenarios, viz., Mrk231. Mrk231 is a Seyfert galaxy that hosts multi-phase multi-scale gas outflows, such as a nuclear ultra-fast outflow (UFO; [103]), a sub-kpc scale HI outflow [104], a kpc-scale molecular CO outflow [34,103], and a  $\sim 3$  kpc scale outflow seen in the Na I doublet lines [35,105]. A massive molecular OH outflow has also been detected in Mrk231 [5,106,107]. In VLA observations, Mrk231 reveals a one-sided radio outflow to the south, comprising a weakly collimated jet

or jet “spine” embedded inside a broader magnetized wind component [108], resembling the stratified radio outflow in III Zw 2 (see Section 4.1). The composite outflow in Mrk231 is curved, low-powered, and oriented at a small angle to our line of sight. The wind component may comprise both a nuclear starburst and AGN wind, where the former may be the primary contributor close to the core, while the latter may dominate further away. Moving away from the core, the wind component could also be the outer layers of a widened jet like a jet “sheath”. The 10-kpc-scale radio structure in Mrk231 is “self-similar” to the radio structure observed on the 10-parsec-scale in the literature (see Figure 1 in [104]), resembling the lobes observed in Mrk6 [48]. The radio structures on the two scales in Mrk231 are not as clearly delineated, however, which may be a result of the low inclination angle. However, the presence of two distinct structures is consistent with episodic jet activity in Mrk231, similar to the case of Mrk6 (see Section 3).

Silpa et al. [108] obtained first-order estimates of the relative contributions of the different components (jet/AGN wind/starburst wind) to the overall budget of the radio emission. While the starburst-driven wind accounted for  $\sim 10\text{--}20\%$  of the total radio emission, both jet and AGN wind contributed significantly to the rest of the emission. To estimate the contribution of starburst-driven wind, two different models were used: one assumed that 10% of the supernova kinetic energy was carried away by the winds [109,110], and the other assumed 40% [111]. The latter analysis has also been carried out assuming two different initial mass functions (IMFs; [112,113]). The contribution of the starburst-driven wind remained the same for the different assumed models. The contribution of AGN wind was estimated assuming two different coupling efficiencies (5%; [88]) and (0.5%; [114]). For a 0.5% coupling efficiency, the radio contribution of the jet estimated using Leitherer et al. [110] model, as well as Dalla Vecchia and Schaye [111] model with Chabrier [113] IMF, turned out to be more than of the wind. Although such a first-order analysis cannot provide a one-to-one correspondence between the dominant driver (between jet or AGN wind) and the outflowing gas phase (HI or Na I D or CO or OH), it still indicates that the multi-phase gas outflow in Mrk231 is likely to be driven by both a jet and a wind.

## 5. Signatures of Jet + Wind Feedback on Parsec-Scales

We now turn our attention to much smaller spatial scales than probed by the GMRT and VLA observations. We focus on the KPNO Internal Spectroscopic Survey Red (KISSR; [115]) sample of Seyfert and LINER galaxies [116]. This sample was chosen based on the presence of double-peaked emission lines in their SDSS spectra as well as a radio detection in the VLA FIRST survey [117]. Phase-referenced observations of this sample with the Very Long Baseline Array (VLBA) have revealed the presence of elongated jet-like features, similar to other Very Long Baseline Interferometry (VLBI) studies of RQ AGN in the literature (e.g., [116,118–123]). Interestingly, these jets are one-sided, similar to the one-sided parsec-scale jets observed in RL AGN. VLBI imaging also reveals one-sided jets in narrow-line Seyfert 1 galaxies [124–126]. A  $\sim 60$  parsec long radio source (jet–core–counterjet) was imaged in the Seyfert 2 galaxy Mrk348 using VLBI by Neff and de Bruyn [127]; the counterjet emission was detected more than 40 parsecs away from the radio core. In RL AGN, one-sidedness is typically understood to be a consequence of Doppler-boosting effects [128]. It is not clear if the one-sidedness in Seyfert or LINER jets is a result of Doppler-boosting effects or due to free-free absorption; multi-frequency and spectral index observations could help to disentangle these two scenarios (e.g., [129,130]). If Doppler-boosting is responsible for the jet one-sidedness in the KISSR sources, for instance, then lower limits to jet speeds would range from  $0.003c$  to  $0.75c$  [116] assuming jet inclinations to be  $\geq 50$  degrees, consistent with their type 2 classification, and the expected torus half-opening angles being  $\sim 50$  degrees (e.g., [131]).

On the other hand, if the missing counterjet emission was a result of free–free absorption, the required electron densities of the ionized gas could be estimated using  $EM = 3.05 \times 10^6 \tau T^{1.35} \nu^{2.1}$ , and  $n_e = \sqrt{EM/l}$  [132], where  $EM$  is the emission measure in  $\text{pc cm}^{-6}$ ,  $\tau$  is the optical depth at frequency  $\nu$  in GHz,  $T$  is the gas temperature in units of  $10^4$  K,  $n_e$  is the electron density in  $\text{cm}^{-3}$ , and  $l$  is the path length in parsecs. In order to account for the observed jet-to-counterjet surface brightness ratios ( $R_J$ ) of  $\sim 20$  on parsec scales (as in the case of KISSR434; [133]), the optical depth at 1.5 GHz would need to be at least  $\sim 1.0$  using  $\exp(-\tau) = 1/R_J$  [134]. For a gas temperature of  $10^4$  K and a jet path length of 1 parsec, an  $EM$  of  $\approx 7.1 \times 10^6 \text{ pc cm}^{-6}$  and  $n_e$  of  $\approx 2700 \text{ cm}^{-3}$  are required for free–free absorption on parsec scales. Such ionized gas densities can be found in NLR gas clouds. However, their volume filling factor is of the order of  $10^{-4}$  (e.g., [135]), making them unlikely candidates for absorbers for the  $\sim 100$ -parsec-scale (counter-)jets observed in a couple of the KISSR sources [116,133]. Ionized gas in giant HII regions with  $n_e \sim 100\text{--}1000 \text{ cm}^{-3}$  could in principle also be the candidate media for free–free absorption [136] but also has a low volume filling factor ( $\geq 0.2$ , e.g., [137]).

Multi-epoch VLBI observations are therefore necessary to check for proper motions and obtain accurate jet speeds to verify the Doppler-boosting picture in Seyferts and LINERs. This has recently become possible for eight KISSR sources. Preliminary results suggest the detection of superluminal jet motion in at least one source (Kharb et al. in prep.). With these new observations, the jet detection rate in the KISSR sample becomes  $\sim 75\%$ . Jet detection rates in larger samples of Seyferts and LINERs range between  $\sim 30\%$  and  $\sim 50\%$  (e.g., [123,138]). The higher jet detection rate in the KISSR sample is consistent with a selection bias that comes from selecting double-peaked emission-line AGN (DPAGN) and jet–NLR interaction being the primary cause of the double-peaked emission lines in them.

Furthermore, it was found that the double peaks of the emission lines were typically separated by velocities of  $\sim 100\text{--}300 \text{ km s}^{-1}$  for most sources, and the widths of the lines corresponded to velocities of  $\sim 100\text{--}200 \text{ km s}^{-1}$  [116,117,133,139]. These velocities are much smaller, by factors of several hundred, than the expected jet speeds. This, therefore, suggests that the emission line gas could be pushed in a direction lateral to the jet (e.g., [33,139]) or could arise in wider, slower-moving winds around the jets (see for example Figure 5). Indeed, nested biconical outflows have been invoked to explain the origin of double-peaked emission lines in low luminosity AGN by Nevin et al. [140,141]. Importantly, wide wind-like outflows can be efficient agents of “AGN feedback” (see the review by [12]). Indeed, from the MAPPINGS III modeling of emission lines such as  $\text{H}\alpha$ ,  $\text{H}\beta$ ,  $\text{H}\gamma$ , [S II], [O III], and [O II], it appears that in sources possessing parsec-scale jets, the “shock + precursor” model can explain the observed line ratios, consistent with the idea of jet–NLR interaction. The “shock + precursor” model comes into play when ionizing radiation (i.e., extreme UV and soft X-ray photons) generated by the cooling of hot gas behind a shock front creates a strong radiation field leading to significant photoionization [142]. The spatial scales sampled by the SDSS optical fiber with a diameter of 3 arcsecs, corresponding to  $\sim 3\text{--}6 \text{ kpc}$  at the distance of the KISSR sources, are much larger than the  $\sim 100$  parsec-scale VLBA jets. However, as Schmitt et al. [143,144] have noted, the NLR ranges from a few 100 parsecs to a few kpcs in Seyfert galaxies. The emission-line modeling is consistent with the idea that RQ AGN are energetically capable of influencing their parsec and kpc-scale environments, making them agents of “radio AGN feedback”.

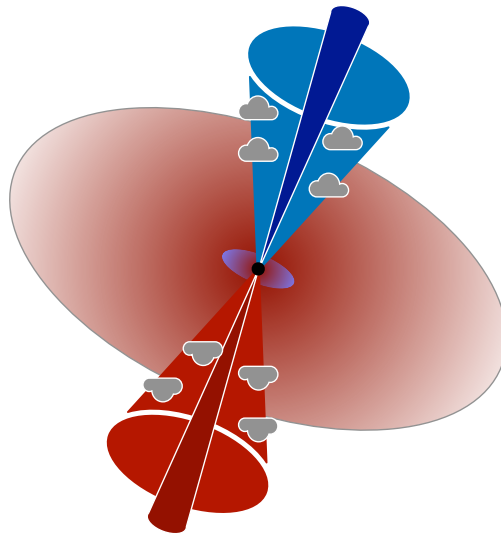


**Figure 5.** Cartoon showing a nested biconical structure in the outflow (that is blue-shifted when approaching and redshifted when receding as denoted by the colors) in order to reproduce the double-peaked emission line AGN spectroscopic observations. The host galaxy (red ellipse) and accretion disk (blue ellipse) as shown here are not to scale. The outer layers of a jet or a wind could be driving the NLR gas clouds.

## 6. Summary

Radio-quiet AGN make up the vast majority of all AGN. While they lack the 100 kpc radio jets and lobes that are observed in the more spectacular looking and rarer radio-loud AGN, the smaller outflows in RQ AGN have profound though subtle effects on their host galaxies. Multi-frequency polarization-sensitive observations of the PG RQ quasars and other Seyfert galaxies with the VLA and GMRT indicate that the radio outflows are layered or stratified. The multi-component outflows could either be spine + sheath structures or jets with winds. While the “sheath” layers around the “spines” of jets could come about due to jet–medium interaction, they continue to entrain the surrounding gas, create instabilities between layers, and further impact both the jet and the medium itself. Small (arcsec) scale jet–medium interaction is also implied by their polarimetric and jet kinetic power data. The picture of nested biconical outflows also emerges from a completely different study, namely, the VLBI study of a sample of Seyfert and LINER galaxies that exhibit double-peaked emission lines in their SDSS optical spectra. Two separate results point to jet–medium interaction in these sources. First, the high incidence of one-sided radio jets, several of which are  $\sim 100$  parsec in extent, points to a selection bias when choosing a DPAGN sample as the double-peaked emission lines appear to be the result of jet–NLR gas cloud interaction. Second, plasma modeling codes on the optical emission lines from SDSS indicate that the NLR gas clouds are affected through the “shock + precursor” mechanism and that the jets are likely stratified with a faster moving “spine” and a slower moving “sheath” or wind. Finally, multi-frequency arcsec-scale observations detect the signatures of multiple jet episodes in RQ AGN through the presence of additional steep-spectrum radio lobes. Episodic AGN activity in fact appears to be the norm in RQ AGN, signatures of which are seen in the radio spectra as well as morphological features like bow-shocks. In the case of the Seyfert galaxies NGC2639 and NGC4051, and others, these multiple jet episodes appear to excavate holes in the molecular gas in the central regions of their host galaxies, consistent with “negative AGN feedback”. However, in many cases, like the PG RQ quasars, there appears to be no currently observable depletion of molecular gas in their host galaxies. “AGN feedback”, therefore, appears to be a complex phenomenon in the

case of RQ AGN. It cannot be ruled out on small spatial scales as implied by the signatures of jet–medium interaction. However, global impact signatures on the host galaxies are often difficult to see.

**Author Contributions:** This paper has contributions from projects lead by both P.K. and S.S. Projects lead by S.S. are a part of her Ph.D. thesis currently being supervised by P.K. All authors have read and agreed to the published version of the manuscript.

**Funding:** This research received no external funding.

**Informed Consent Statement:** Informed consent was obtained from all subjects involved in the study.

**Data Availability Statement:** The data underlying this article will be shared on reasonable request to the corresponding author.

**Acknowledgments:** We thank the anonymous reviewers for their suggestions that have significantly improved this paper. We thank the staff of the GMRT that made these observations possible. GMRT is run by the National Center for Radio Astrophysics of the Tata Institute of Fundamental Research. P.K. and S.S. acknowledge the support of the Department of Atomic Energy, Government of India, under the project 12-R&D-TFR-5.02-0700. The National Radio Astronomy Observatory is a facility of the National Science Foundation operated under cooperative agreement by Associated Universities, Inc.

**Conflicts of Interest:** The authors declare no conflict of interest.

## Note

<sup>1</sup> [https://webarchive.gemini.edu/20210427-gsm12/gsm2012\\_poster\\_may-daniel.pdf](https://webarchive.gemini.edu/20210427-gsm12/gsm2012_poster_may-daniel.pdf) (accessed on 1 January 2023).

## References

- Gardner, J.P.; Mather, J.C.; Clampin, M.; Doyon, R.; Greenhouse, M.A.; Hammel, H.B.; Hutchings, J.B.; Jakobsen, P.; Lilly, S.J.; Long, K.S.; et al. The James Webb Space Telescope. *Space Sci. Rev.* **2006**, *123*, 485–606. [[CrossRef](#)]
- Fabian, A.C. Observational Evidence of Active Galactic Nuclei Feedback. *Annu. Rev. Astron. Astrophys.* **2012**, *50*, 455–489. [[CrossRef](#)]
- King, A.; Pounds, K. Powerful Outflows and Feedback from Active Galactic Nuclei. *Annu. Rev. Astron. Astrophys.* **2015**, *53*, 115–154. [[CrossRef](#)]
- Alexander, D.M.; Hickox, R.C. What drives the growth of black holes? *New Astron. Rev.* **2012**, *56*, 93–121. [[CrossRef](#)]
- Morganti, R. The many routes to AGN feedback. *Front. Astron. Space Sci.* **2017**, *4*, 42. [[CrossRef](#)]
- Harrison, C.M. Impact of supermassive black hole growth on star formation. *Nat. Astron.* **2017**, *1*, 0165. [[CrossRef](#)]
- Faucher-Giguère, C.A.; Quataert, E. The physics of galactic winds driven by active galactic nuclei. *Mon. Not. R. Astron. Soc.* **2012**, *425*, 605–622. [[CrossRef](#)]
- Costa, T.; Rosdahl, J.; Sijacki, D.; Haehnelt, M.G. Quenching star formation with quasar outflows launched by trapped IR radiation. *Mon. Not. R. Astron. Soc.* **2018**, *479*, 2079–2111. [[CrossRef](#)]
- McNamara, B.R.; Nulsen, P.E.J. Mechanical feedback from active galactic nuclei in galaxies, groups and clusters. *New J. Phys.* **2012**, *14*, 055023. [[CrossRef](#)]
- Mahony, E.K.; Morganti, R.; Emonts, B.H.C.; Oosterloo, T.A.; Tadhunter, C. The location and impact of jet-driven outflows of cold gas: The case of 3C 293. *Mon. Not. R. Astron. Soc.* **2013**, *435*, L58–L62. [[CrossRef](#)]
- Hardcastle, M.J.; Croston, J.H. Radio galaxies and feedback from AGN jets. *New Astron. Rev.* **2020**, *88*, 101539. [[CrossRef](#)]
- Harrison, C.M.; Costa, T.; Tadhunter, C.N.; Flütsch, A.; Kakkad, D.; Perna, M.; Vietri, G. AGN outflows and feedback twenty years on. *Nat. Astron.* **2018**, *2*, 198–205. [[CrossRef](#)]
- de Bruyn, A.G.; Wilson, A.S. A 1415 MHz Survey of Seyfert and Related Galaxies. *Astron. Astrophys.* **1976**, *53*, 93.
- Ulvestad, J.S.; Wilson, A.S. Radio structures of Seyfert galaxies. VI. VLA observations of a nearby sample. *Astrophys. J.* **1984**, *285*, 439–452. [[CrossRef](#)]
- Roy, A.L.; Norris, R.P.; Kesteven, M.J.; Troup, E.R.; Reynolds, J.E. Compact Radio Cores in Seyfert Galaxies. *Astrophys. J.* **1994**, *432*, 496. [[CrossRef](#)]
- Thean, A.; Pedlar, A.; Kukula, M.J.; Baum, S.A.; O’Dea, C.P. High-resolution radio observations of Seyfert galaxies in the extended 12- $\mu$ m sample—II. The properties of compact radio components. *Mon. Not. R. Astron. Soc.* **2001**, *325*, 737–760. [[CrossRef](#)]
- Gallimore, J.F.; Axon, D.J.; O’Dea, C.P.; Baum, S.A.; Pedlar, A. A Survey of Kiloparsec-Scale Radio Outflows in Radio-Quiet Active Galactic Nuclei. *Astron. J.* **2006**, *132*, 546–569. [[CrossRef](#)]
- Singh, V.; Ishwara-Chandra, C.H.; Wadadekar, Y.; Beelen, A.; Kharb, P. Kiloparsec-scale radio emission in Seyfert and LINER galaxies. *Mon. Not. R. Astron. Soc.* **2015**, *446*, 599–612. [[CrossRef](#)]
- Kellermann, K.I.; Sramek, R.; Schmidt, M.; Shaffer, D.B.; Green, R. VLA Observations of Objects in the Palomar Bright Quasar Survey. *Astron. J.* **1989**, *98*, 1195. [[CrossRef](#)]
- Kellermann, K.I.; Condon, J.J.; Kimball, A.E.; Perley, R.A.; Ivezić, Ž. Radio-loud and Radio-quiet QSOs. *Astrophys. J.* **2016**, *831*, 168. [[CrossRef](#)]
- Heckman, T.M. An Optical and Radio Survey of the Nuclei of Bright Galaxies - Activity in the Normal Galactic Nuclei. *Astron. Astrophys.* **1980**, *87*, 152.
- Ho, L.C. Nuclear Activity in Nearby Galaxies. *Annu. Rev. Astron. Astrophys.* **2008**, *46*, 475–539. [[CrossRef](#)]
- Ho, L.C. LINERs as low-luminosity active galactic nuclei. *Adv. Space Res.* **1999**, *23*, 813–822. [[CrossRef](#)]
- Ho, L.C. Radiatively Inefficient Accretion in Nearby Galaxies. *Astrophys. J.* **2009**, *699*, 626–637. [[CrossRef](#)]
- Venturi, G.; Cresci, G.; Marconi, A.; Mingozzi, M.; Nardini, E.; Carniani, S.; Mannucci, F.; Marasco, A.; Maiolino, R.; Perna, M.; et al. MAGNUM survey: Compact jets causing large turmoil in galaxies. Enhanced line widths perpendicular to radio jets as tracers of jet-ISM interaction. *Astron. Astrophys.* **2021**, *648*, A17. [[CrossRef](#)]
- Tadhunter, C.; Morganti, R.; Rose, M.; Oonk, J.B.R.; Oosterloo, T. Jet acceleration of the fast molecular outflows in the Seyfert galaxy IC 5063. *Nature* **2014**, *511*, 440–443. [[CrossRef](#)]
- Dasyra, K.M.; Paraschos, G.F.; Bisbas, T.G.; Combes, F.; Fernández-Ontiveros, J.A. Insights into the collapse and expansion of molecular clouds in outflows from observable pressure gradients. *Nat. Astron.* **2022**, *6*, 1077–1084. [[CrossRef](#)]
- Alatalo, K.; Blitz, L.; Young, L.M.; Davis, T.A.; Bureau, M.; Lopez, L.A.; Cappellari, M.; Scott, N.; Shapiro, K.L.; Crocker, A.F.; et al. Discovery of an Active Galactic Nucleus Driven Molecular Outflow in the Local Early-type Galaxy NGC 1266. *Astrophys. J.* **2011**, *735*, 88. [[CrossRef](#)]

29. Singha, M. The Curious Case of a Radio Quiet AGN: Jet-Outflow Connection Unveiled by the Close AGN Reference Survey (CARS). In Proceedings of the Multiphase AGN Feeding & Feedback II, Sexten, Italy, 20–24 June 2022; p. 59.
30. Jarvis, M.E.; Harrison, C.M.; Thomson, A.P.; Circosta, C.; Mainieri, V.; Alexander, D.M.; Edge, A.C.; Lansbury, G.B.; Molyneux, S.J.; Mullaney, J.R. Prevalence of radio jets associated with galactic outflows and feedback from quasars. *Mon. Not. R. Astron. Soc.* **2019**, *485*, 2710–2730. [[CrossRef](#)]
31. Girdhar, A. The Important Role of Low Power Radio Jets in Driving Multiphase Outflows in Quasar Host Galaxies. In Proceedings of the Multiphase AGN Feeding & Feedback II, Sexten, Italy, 20–24 June 2022; p. 20.
32. Silpa, S.; Kharb, P.; Harrison, C.M.; Girdhar, A.; Mukherjee, D.; Mainieri, V.; Jarvis, M.E. The Quasar Feedback Survey: Revealing the interplay of jets, winds, and emission-line gas in type 2 quasars with radio polarization. *Mon. Not. R. Astron. Soc.* **2022**, *513*, 4208–4223. [[CrossRef](#)]
33. Girdhar, A.; Harrison, C.M.; Mainieri, V.; Bittner, A.; Costa, T.; Kharb, P.; Mukherjee, D.; Arrigoni Battaia, F.; Alexander, D.M.; Calistro Rivera, G.; et al. Quasar feedback survey: Multiphase outflows, turbulence, and evidence for feedback caused by low power radio jets inclined into the galaxy disc. *Mon. Not. R. Astron. Soc.* **2022**, *512*, 1608–1628. [[CrossRef](#)]
34. Feruglio, C.; Maiolino, R.; Piconcelli, E.; Menci, N.; Aussel, H.; Lamastra, A.; Fiore, F. Quasar feedback revealed by giant molecular outflows. *Astron. Astrophys.* **2010**, *518*, L155. [[CrossRef](#)]
35. Rupke, D.S.N.; Veilleux, S. Integral Field Spectroscopy of Massive, Kiloparsec-scale Outflows in the Infrared-luminous QSO Mrk 231. *Astrophys. J. Lett.* **2011**, *729*, L27. [[CrossRef](#)]
36. Liu, G.; Zakamska, N.L.; Greene, J.E.; Nesvadba, N.P.H.; Liu, X. Observations of feedback from radio-quiet quasars—II. Kinematics of ionized gas nebulae. *Mon. Not. R. Astron. Soc.* **2013**, *436*, 2576–2597. [[CrossRef](#)]
37. Zakamska, N.L.; Greene, J.E. Quasar feedback and the origin of radio emission in radio-quiet quasars. *Mon. Not. R. Astron. Soc.* **2014**, *442*, 784–804. [[CrossRef](#)]
38. McElroy, R.; Croom, S.M.; Pracy, M.; Sharp, R.; Ho, I.T.; Medling, A.M. IFU observations of luminous type II AGN—I. Evidence for ubiquitous winds. *Mon. Not. R. Astron. Soc.* **2015**, *446*, 2186–2204. [[CrossRef](#)]
39. Wylezalek, D.; Zakamska, N.L. Evidence of suppression of star formation by quasar-driven winds in gas-rich host galaxies at  $z < 1$ ? *Mon. Not. R. Astron. Soc.* **2016**, *461*, 3724–3739. [[CrossRef](#)]
40. Kharb, P.; Srivastava, S.; Singh, V.; Gallimore, J.F.; Ishwara-Chandra, C.H.; Ananda, H. A GMRT study of Seyfert galaxies NGC 4235 and NGC 4594: Evidence of episodic activity? *Mon. Not. R. Astron. Soc.* **2016**, *459*, 1310–1326. [[CrossRef](#)]
41. Singh, V.; Shastri, P.; Ishwara-Chandra, C.H.; Athreya, R. Low-frequency radio observations of Seyfert galaxies: A test of the unification scheme. *Astron. Astrophys.* **2013**, *554*, A85. [[CrossRef](#)]
42. Hota, A.; Saikia, D.J. Radio bubbles in the composite AGN-starburst galaxy NGC6764. *Mon. Not. R. Astron. Soc.* **2006**, *371*, 945–956. [[CrossRef](#)]
43. Silpa, S.; Kharb, P.; Ho, L.C.; Ishwara-Chandra, C.H.; Jarvis, M.E.; Harrison, C. Probing the origin of low-frequency radio emission in PG quasars with the uGMRT—I. *Mon. Not. R. Astron. Soc.* **2020**, *499*, 5826–5839. [[CrossRef](#)]
44. Silpa, S.; Kharb, P.; Harrison, C.M.; Ho, L.C.; Jarvis, M.E.; Ishwara-Chandra, C.H.; Sebastian, B. Outflows in the radio-intermediate quasar III Zw 2: A polarization study with the EVLA and uGMRT. *Mon. Not. R. Astron. Soc.* **2021**, *507*, 991–1001. [[CrossRef](#)]
45. Rao, V.V.; Kharb, P.; Rubinur, K.; Silpa, S.; Roy, N.; Sebastian, B.; Singh, V.; Baghel, J.; Manna, S.; Ishwara-Chandra, C.H. AGN Feedback Through Multiple Jet Cycles in the Seyfert Galaxy NGC 2639. *arXiv* **2023**, arXiv:2301.01610.
46. Roettiger, K.; Burns, J.O.; Clarke, D.A.; Christiansen, W.A. Relic radio emission in 3C 388. *Astrophys. J.* **1994**, *421*, L23–L26. [[CrossRef](#)]
47. Sanders, R.H. Seyfert nuclei as short-lived stochastic accretion events. *Astron. Astrophys.* **1984**, *140*, 52–54.
48. Kharb, P.; O’Dea, C.P.; Baum, S.A.; Colbert, E.J.M.; Xu, C. A Radio Study of the Seyfert Galaxy Markarian 6: Implications for Seyfert Life Cycles. *Astrophys. J.* **2006**, *652*, 177–188. [[CrossRef](#)]
49. Irwin, J.A.; Schmidt, P.; Damas-Segovia, A.; Beck, R.; English, J.; Heald, G.; Henriksen, R.N.; Krause, M.; Li, J.T.; Rand, R.J.; et al. CHANG-ES—VIII. Uncovering hidden AGN activity in radio polarization. *Mon. Not. R. Astron. Soc.* **2016**, *464*, 1333–1346. [[CrossRef](#)]
50. Sebastian, B.; Kharb, P.; O’Dea, C.P.; Gallimore, J.F.; Baum, S.A. The discovery of secondary lobes in the Seyfert galaxy NGC 2639. *Mon. Not. R. Astron. Soc.* **2019**, *490*, L26–L31. [[CrossRef](#)]
51. Sebastian, B.; Kharb, P.; O’Dea, C.P.; Gallimore, J.F.; Baum, S.A. A radio polarimetric study to disentangle AGN activity and star formation in Seyfert galaxies. *Mon. Not. R. Astron. Soc.* **2020**, *499*, 334–354. [[CrossRef](#)]
52. Jurlin, N.; Morganti, R.; Brienza, M.; Mandal, S.; Maddox, N.; Duncan, K.J.; Shabala, S.S.; Hardcastle, M.J.; Prandoni, I.; Röttgering, H.J.A.; et al. The life cycle of radio galaxies in the LOFAR Lockman Hole field. *Astron. Astrophys.* **2020**, *638*, A34. [[CrossRef](#)]
53. Lalakos, A.; Gottlieb, O.; Kaaz, N.; Chatterjee, K.; Liska, M.; Christie, I.M.; Tchekhovskoy, A.; Zhuravleva, I.; Nokhrina, E. Bridging the Bondi and Event Horizon Scales: 3D GRMHD Simulations Reveal X-shaped Radio Galaxy Morphology. *Astrophys. J.* **2022**, *936*, L5. [[CrossRef](#)]
54. Harwood, J.J.; Hardcastle, M.J.; Croston, J.H. Spectral ageing in the lobes of cluster-centre FR II radio galaxies. *Mon. Not. R. Astron. Soc.* **2015**, *454*, 3403–3422. [[CrossRef](#)]

55. Bolatto, A.D.; Wong, T.; Utomo, D.; Blitz, L.; Vogel, S.N.; Sánchez, S.F.; Barrera-Ballesteros, J.; Cao, Y.; Colombo, D.; Dannerbauer, H.; et al. The EDGE-CALIFA Survey: Interferometric Observations of 126 Galaxies with CARMA. *Astrophys. J.* **2017**, *846*, 159. [[CrossRef](#)]
56. Sánchez, S.F.; Kennicutt, R.C.; Gil de Paz, A.; van de Ven, G.; Vílchez, J.M.; Wisotzki, L.; Walcher, C.J.; Mast, D.; Aguerri, J.A.L.; Albiol-Pérez, S.; et al. CALIFA, the Calar Alto Legacy Integral Field Area survey. I. Survey presentation. *Astron. Astrophys.* **2012**, *538*, A8. [[CrossRef](#)]
57. Ellison, S.L.; Wong, T.; Sánchez, S.F.; Colombo, D.; Bolatto, A.; Barrera-Ballesteros, J.; García-Benito, R.; Kalinova, V.; Luo, Y.; Rubio, M.; et al. The EDGE-CALIFA survey: Central molecular gas depletion in AGN host galaxies—A smoking gun for quenching? *Mon. Not. R. Astron. Soc.* **2021**, *505*, L46–L51. [[CrossRef](#)]
58. Merloni, A.; Heinz, S. Measuring the kinetic power of active galactic nuclei in the radio mode. *Mon. Not. R. Astron. Soc.* **2007**, *381*, 589–601. [[CrossRef](#)]
59. Jones, S.; McHardy, I.; Moss, D.; Seymour, N.; Breedt, E.; Uttley, P.; Körding, E.; Tudose, V. Radio and X-ray variability in the Seyfert galaxy NGC 4051. *Mon. Not. R. Astron. Soc.* **2011**, *412*, 2641–2652. [[CrossRef](#)]
60. Giroletti, M.; Panessa, F. The Faintest Seyfert Radio Cores Revealed by VLBI. *Astrophys. J.* **2009**, *706*, L260–L264. [[CrossRef](#)]
61. Riffel, R.A.; Storchi-Bergmann, T.; Winge, C.; McGregor, P.J.; Beck, T.; Schmitt, H. Mapping of molecular gas inflow towards the Seyfert nucleus of NGC4051 using Gemini NIFS. *Mon. Not. R. Astron. Soc.* **2008**, *385*, 1129–1142. [[CrossRef](#)]
62. Boroson, T.A.; Green, R.F. The Emission-Line Properties of Low-Redshift Quasi-stellar Objects. *Astrophys. J. Suppl. Ser.* **1992**, *80*, 109. [[CrossRef](#)]
63. Silpa, S.; Kharb, P.; Ho, L.C.; Harrison, C.M. A Radio-Gas Study of 11 Radio-quiet PG Quasars. *arXiv* **2023**, arXiv:2301.07929.
64. Mehdipour, M.; Costantini, E. Relation between winds and jets in radio-loud AGN. *Astron. Astrophys.* **2019**, *625*, A25. [[CrossRef](#)]
65. Miller, J.M.; Raymond, J.; Fabian, A.C.; Reynolds, C.S.; King, A.L.; Kallman, T.R.; Cackett, E.M.; van der Klis, M.; Steeghs, D.T.H. The Disk-wind-Jet Connection in the Black Hole H 1743-322. *Astrophys. J.* **2012**, *759*, L6. [[CrossRef](#)]
66. Komissarov, S.S. Mass-Loaded Relativistic Jets. *Mon. Not. R. Astron. Soc.* **1994**, *269*, 394. [[CrossRef](#)]
67. Bowman, M.; Leahy, J.P.; Komissarov, S.S. The deceleration of relativistic jets by entrainment. *Mon. Not. R. Astron. Soc.* **1996**, *279*, 899. [[CrossRef](#)]
68. Perucho, M.; Martí, J.M. A numerical simulation of the evolution and fate of a Fanaroff-Riley type I jet. The case of 3C 31. *Mon. Not. R. Astron. Soc.* **2007**, *382*, 526–542. [[CrossRef](#)]
69. Perucho, M.; Martí, J.M.; Laing, R.A.; Hardee, P.E. On the deceleration of Fanaroff-Riley Class I jets: Mass loading by stellar winds. *Mon. Not. R. Astron. Soc.* **2014**, *441*, 1488–1503. [[CrossRef](#)]
70. Hardee, P.E. Spatial Stability of Relativistic Jets: Application to 3C 345. *Astrophys. J.* **1987**, *318*, 78. [[CrossRef](#)]
71. Savolainen, T.; Wiik, K.; Valtaoja, E.; Kadler, M.; Ros, E.; Tornikoski, M.; Aller, M.F.; Aller, H.D. An Extremely Curved Relativistic Jet in PKS 2136+141. *Astrophys. J.* **2006**, *647*, 172–184. [[CrossRef](#)]
72. Mukherjee, D.; Bodo, G.; Mignone, A.; Rossi, P.; Vaidya, B. Simulating the dynamics and non-thermal emission of relativistic magnetized jets I. Dynamics. *Mon. Not. R. Astron. Soc.* **2020**, *499*, 681–701. [[CrossRef](#)]
73. Shangguan, J.; Ho, L.C.; Bauer, F.E.; Wang, R.; Treister, E. AGN Feedback and Star Formation of Quasar Host Galaxies: Insights from the Molecular Gas. *Astrophys. J.* **2020**, *899*, 112. [[CrossRef](#)]
74. Kennicutt, R.C., Jr. The Global Schmidt Law in Star-forming Galaxies. *Astrophys. J.* **1998**, *498*, 541–552. [[CrossRef](#)]
75. Molina, J.; Ho, L.C.; Wang, R.; Shangguan, J.; Bauer, F.E.; Treister, E.; Zhuang, M.Y.; Ricci, C.; Bian, F. Ionized Outflows in Nearby Quasars Are Poorly Coupled to Their Host Galaxies. *Astrophys. J.* **2022**, *935*, 72. [[CrossRef](#)]
76. Jarvis, M.E.; Harrison, C.M.; Mainieri, V.; Calistro Rivera, G.; Jethwa, P.; Zhang, Z.Y.; Alexander, D.M.; Circosta, C.; Costa, T.; De Breuck, C.; et al. High molecular gas content and star formation rates in local galaxies that host quasars, outflows, and jets. *Mon. Not. R. Astron. Soc.* **2020**, *498*, 1560–1575. [[CrossRef](#)]
77. van der Werf, P.P.; Isaak, K.G.; Meijerink, R.; Spaans, M.; Rykala, A.; Fulton, T.; Loenen, A.F.; Walter, F.; Weiß, A.; Armus, L.; et al. Black hole accretion and star formation as drivers of gas excitation and chemistry in Markarian 231. *Astron. Astrophys.* **2010**, *518*, L42. [[CrossRef](#)]
78. Mashian, N.; Sturm, E.; Sternberg, A.; Janssen, A.; Hailey-Dunsheath, S.; Fischer, J.; Contursi, A.; González-Alfonso, E.; Graciá-Carpio, J.; Poglitsch, A.; et al. High-J CO Sleds in Nearby Infrared Bright Galaxies Observed By Herschel/PACS. *Astrophys. J.* **2015**, *802*, 81. [[CrossRef](#)]
79. Carniani, S.; Gallerani, S.; Vallini, L.; Pallottini, A.; Tazzari, M.; Ferrara, A.; Maiolino, R.; Cicone, C.; Feruglio, C.; Neri, R.; et al. Constraints on high-J CO emission lines in  $z \sim 6$  quasars. *Mon. Not. R. Astron. Soc.* **2019**, *489*, 3939–3952. [[CrossRef](#)]
80. Dasyra, K.M.; Combes, F.; Oosterloo, T.; Oonk, J.B.R.; Morganti, R.; Salomé, P.; Vlahakis, N. ALMA reveals optically thin, highly excited CO gas in the jet-driven winds of the galaxy IC 5063. *Astron. Astrophys.* **2016**, *595*, L7. [[CrossRef](#)]
81. Zhang, C.P.; Li, G.X.; Zhou, C.; Yuan, L.; Zhu, M. Using CO line ratios to trace compressed areas in bubble N131. *Astron. Astrophys.* **2019**, *631*, A110. [[CrossRef](#)]
82. Salomé, Q.; Salomé, P.; Miville-Deschênes, M.A.; Combes, F.; Hamer, S. Inefficient jet-induced star formation in Centaurus A. High resolution ALMA observations of the northern filaments. *Astron. Astrophys.* **2017**, *608*, A98. [[CrossRef](#)]

83. Rosario, D.J.; Burtscher, L.; Davies, R.I.; Koss, M.; Ricci, C.; Lutz, D.; Riffel, R.; Alexander, D.M.; Genzel, R.; Hicks, E.H.; et al. LLAMA: Normal star formation efficiencies of molecular gas in the centres of luminous Seyfert galaxies. *Mon. Not. R. Astron. Soc.* **2018**, *473*, 5658–5679. [[CrossRef](#)]
84. Fotopoulou, C.M.; Dasyra, K.M.; Combes, F.; Salomé, P.; Papachristou, M. Complex molecular gas kinematics in the inner 5 kpc of 4C12.50 as seen by ALMA. *Astron. Astrophys.* **2019**, *629*, A30. [[CrossRef](#)]
85. Ramakrishnan, V.; Nagar, N.M.; Finlez, C.; Storchi-Bergmann, T.; Slater, R.; Schnorr-Müller, A.; Riffel, R.A.; Mundell, C.G.; Robinson, A. Nuclear kinematics in nearby AGN—I. An ALMA perspective on the morphology and kinematics of the molecular CO(2-1) emission. *Mon. Not. R. Astron. Soc.* **2019**, *487*, 444–455. [[CrossRef](#)]
86. Shin, J.; Woo, J.H.; Chung, A.; Baek, J.; Cho, K.; Kang, D.; Bae, H.J. Positive and Negative Feedback of AGN Outflows in NGC 5728. *Astrophys. J.* **2019**, *881*, 147. [[CrossRef](#)]
87. Lutz, D.; Sturm, E.; Janssen, A.; Veilleux, S.; Aalto, S.; Cicone, C.; Contursi, A.; Davies, R.I.; Feruglio, C.; Fischer, J.; et al. Molecular outflows in local galaxies: Method comparison and a role of intermittent AGN driving. *Astron. Astrophys.* **2020**, *633*, A134. [[CrossRef](#)]
88. Di Matteo, T.; Springel, V.; Hernquist, L. Energy input from quasars regulates the growth and activity of black holes and their host galaxies. *Nature* **2005**, *433*, 604–607. [[CrossRef](#)]
89. Springel, V.; Di Matteo, T.; Hernquist, L. Black Holes in Galaxy Mergers: The Formation of Red Elliptical Galaxies. *Astrophys. J.* **2005**, *620*, L79–L82. [[CrossRef](#)]
90. Cox, T.J.; Jonsson, P.; Primack, J.R.; Somerville, R.S. Feedback in simulations of disc-galaxy major mergers. *Mon. Not. R. Astron. Soc.* **2006**, *373*, 1013–1038. [[CrossRef](#)]
91. Hopkins, P.F.; Cox, T.J.; Kereš, D.; Hernquist, L. A Cosmological Framework for the Co-Evolution of Quasars, Supermassive Black Holes, and Elliptical Galaxies. II. Formation of Red Ellipticals. *Astrophys. J. Suppl. Ser.* **2008**, *175*, 390–422. [[CrossRef](#)]
92. Khalatyan, A.; Cattaneo, A.; Schramm, M.; Gottlöber, S.; Steinmetz, M.; Wisotzki, L. Is AGN feedback necessary to form red elliptical galaxies? *Mon. Not. R. Astron. Soc.* **2008**, *387*, 13–30. [[CrossRef](#)]
93. Cheung, E.; Faber, S.M.; Koo, D.C.; Dutton, A.A.; Simard, L.; McGrath, E.J.; Huang, J.S.; Bell, E.F.; Dekel, A.; Fang, J.J.; et al. The Dependence of Quenching upon the Inner Structure of Galaxies at  $0.5 \leq z < 0.8$  in the DEEP2/AEGIS Survey. *Astrophys. J.* **2012**, *760*, 131. [[CrossRef](#)]
94. Barro, G.; Faber, S.M.; Pérez-González, P.G.; Koo, D.C.; Williams, C.C.; Kocevski, D.D.; Trump, J.R.; Mozena, M.; McGrath, E.; van der Wel, A.; et al. CANDELS: The Progenitors of Compact Quiescent Galaxies at  $z \sim 2$ . *Astrophys. J.* **2013**, *765*, 104. [[CrossRef](#)]
95. Smethurst, R.J.; Lintott, C.J.; Simmons, B.D.; Schawinski, K.; Marshall, P.J.; Bamford, S.; Fortson, L.; Kaviraj, S.; Masters, K.L.; Melvin, T.; et al. Galaxy Zoo: Evidence for diverse star formation histories through the green valley. *Mon. Not. R. Astron. Soc.* **2015**, *450*, 435–453. [[CrossRef](#)]
96. Springel, V.; Di Matteo, T.; Hernquist, L. Modelling feedback from stars and black holes in galaxy mergers. *Mon. Not. R. Astron. Soc.* **2005**, *361*, 776–794. [[CrossRef](#)]
97. Sanders, D.B.; Mirabel, I.F. Luminous Infrared Galaxies. *Annu. Rev. Astron. Astrophys.* **1996**, *34*, 749. [[CrossRef](#)]
98. Mihos, J.C.; Hernquist, L. Gasdynamics and Starbursts in Major Mergers. *Astrophys. J.* **1996**, *464*, 641. [[CrossRef](#)]
99. Lin, L.; Koo, D.C.; Weiner, B.J.; Chiueh, T.; Coil, A.L.; Lotz, J.; Conselice, C.J.; Willner, S.P.; Smith, H.A.; Guhathakurta, P.; et al. AEGIS: Enhancement of Dust-enshrouded Star Formation in Close Galaxy Pairs and Merging Galaxies up to  $z \sim 1$ . *Astrophys. J.* **2007**, *660*, L51–L54. [[CrossRef](#)]
100. Mahoro, A.; Pović, M.; Nkundabakura, P. Star formation of far-IR AGN and non-AGN galaxies in the green valley: Possible implication of AGN positive feedback. *Mon. Not. R. Astron. Soc.* **2017**, *471*, 3226–3233. [[CrossRef](#)]
101. Mahoro, A.; Pović, M.; Nkundabakura, P.; Nyiransengiyumva, B.; Väisänen, P. Star formation in far-IR AGN and non-AGN galaxies in the green valley—II. Morphological analysis. *Mon. Not. R. Astron. Soc.* **2019**, *485*, 452–463. [[CrossRef](#)]
102. Weigel, A.K.; Schawinski, K.; Caplar, N.; Carpineti, A.; Hart, R.E.; Kaviraj, S.; Keel, W.C.; Kruk, S.J.; Lintott, C.J.; Nichol, R.C.; et al. Galaxy Zoo: Major Galaxy Mergers Are Not a Significant Quenching Pathway. *Astrophys. J.* **2017**, *845*, 145. [[CrossRef](#)]
103. Feruglio, C.; Fiore, F.; Carniani, S.; Piconcelli, E.; Zappacosta, L.; Bongiorno, A.; Cicone, C.; Maiolino, R.; Marconi, A.; Menci, N.; et al. The multi-phase winds of Markarian 231: From the hot, nuclear, ultra-fast wind to the galaxy-scale, molecular outflow. *Astron. Astrophys.* **2015**, *583*, A99. [[CrossRef](#)]
104. Morganti, R.; Veilleux, S.; Oosterloo, T.; Teng, S.H.; Rupke, D. Another piece of the puzzle: The fast H I outflow in Mrk 231. *Astron. Astrophys.* **2016**, *593*, A30. [[CrossRef](#)]
105. Rupke, D.S.N.; Veilleux, S. The Multiphase Structure and Power Sources of Galactic Winds in Major Mergers. *Astrophys. J.* **2013**, *768*, 75. [[CrossRef](#)]
106. Fischer, J.; Sturm, E.; González-Alfonso, E.; Graciá-Carpio, J.; Hailey-Dunsheath, S.; Poglitsch, A.; Contursi, A.; Lutz, D.; Genzel, R.; Sternberg, A.; et al. Herschel-PACS spectroscopic diagnostics of local ULIRGs: Conditions and kinematics in Markarian 231. *Astron. Astrophys.* **2010**, *518*, L41. [[CrossRef](#)]

107. Sturm, E.; González-Alfonso, E.; Veilleux, S.; Fischer, J.; Graciá-Carpio, J.; Hailey-Dunsheath, S.; Contursi, A.; Poglitsch, A.; Sternberg, A.; Davies, R.; et al. Massive Molecular Outflows and Negative Feedback in ULIRGs Observed by Herschel-PACS. *Astrophys. J.* **2011**, *733*, L16. [[CrossRef](#)]
108. Silpa, S.; Kharb, P.; O’Dea, C.P.; Baum, S.A.; Sebastian, B.; Mukherjee, D.; Harrison, C.M. AGN jets and winds in polarized light: The case of Mrk 231. *Mon. Not. R. Astron. Soc.* **2021**, *507*, 2550–2561. [[CrossRef](#)]
109. Thornton, K.; Gaudlitz, M.; Janka, H.T.; Steinmetz, M. Energy Input and Mass Redistribution by Supernovae in the Interstellar Medium. *Astrophys. J.* **1998**, *500*, 95–119. [[CrossRef](#)]
110. Leitherer, C.; Schaerer, D.; Goldader, J.D.; Delgado, R.M.G.; Robert, C.; Kune, D.F.; de Mello, D.F.; Devost, D.; Heckman, T.M. Starburst99: Synthesis Models for Galaxies with Active Star Formation. *Astrophys. J. Suppl. Ser.* **1999**, *123*, 3–40. [[CrossRef](#)]
111. Dalla Vecchia, C.; Schaye, J. Simulating galactic outflows with kinetic supernova feedback. *Mon. Not. R. Astron. Soc.* **2008**, *387*, 1431–1444. [[CrossRef](#)]
112. Salpeter, E.E. The Luminosity Function and Stellar Evolution. *Astrophys. J.* **1955**, *121*, 161. [[CrossRef](#)]

113. Chabrier, G. Galactic Stellar and Substellar Initial Mass Function. *Publ. Astron. Soc. Pac.* **2003**, *115*, 763–795. [[CrossRef](#)]
114. Hopkins, P.F.; Elvis, M. Quasar feedback: More bang for your buck. *Mon. Not. R. Astron. Soc.* **2010**, *401*, 7–14. [[CrossRef](#)]
115. Wegner, G.; Salzer, J.J.; Jangren, A.; Gronwall, C.; Melbourne, J. Spectroscopy of KISS Emission-Line Galaxy Candidates. I. MDM Observations. *Astron. J.* **2003**, *125*, 2373–2392. [[CrossRef](#)]
116. Kharb, P.; Subramanian, S.; Das, M.; Vaddi, S.; Paragi, Z. The Nature of Jets in Double-peaked Emission-line AGN in the KISSR Sample. *Astrophys. J.* **2021**, *919*, 108. [[CrossRef](#)]
117. Kharb, P.; Das, M.; Paragi, Z.; Subramanian, S.; Chitta, L.P. VLBI Imaging of the Double Peaked Emission Line Seyfert KISSR 1494. *Astrophys. J.* **2015**, *799*, 161. [[CrossRef](#)]
118. Falcke, H.; Nagar, N.M.; Wilson, A.S.; Ulvestad, J.S. Radio Sources in Low-Luminosity Active Galactic Nuclei. II. Very Long Baseline Interferometry Detections of Compact Radio Cores and Jets in a Sample of LINERs. *Astrophys. J.* **2000**, *542*, 197–200. [[CrossRef](#)]
119. Middelberg, E.; Roy, A.L.; Nagar, N.M.; Krichbaum, T.P.; Norris, R.P.; Wilson, A.S.; Falcke, H.; Colbert, E.J.M.; Witzel, A.; Fricke, K.J. Motion and properties of nuclear radio components in Seyfert galaxies seen with VLBI. *Astron. Astrophys.* **2004**, *417*, 925–944. [[CrossRef](#)]
120. Nagar, N.M.; Falcke, H.; Wilson, A.S. Radio sources in low-luminosity active galactic nuclei. IV. Radio luminosity function, importance of jet power, and radio properties of the complete Palomar sample. *Astron. Astrophys.* **2005**, *435*, 521–543. [[CrossRef](#)]
121. Kharb, P.; Hota, A.; Croston, J.H.; Hardcastle, M.J.; O’Dea, C.P.; Kraft, R.P.; Axon, D.J.; Robinson, A. Parsec-scale Imaging of the Radio-bubble Seyfert Galaxy NGC 6764. *Astrophys. J.* **2010**, *723*, 580–586. [[CrossRef](#)]
122. Orienti, M.; Prieto, M.A. Radio structures of the nuclei of nearby Seyfert galaxies and the nature of the missing diffuse emission. *Mon. Not. R. Astron. Soc.* **2010**, *401*, 2599–2610. [[CrossRef](#)]
123. Baldi, R.D.; Williams, D.R.A.; McHardy, I.M.; Beswick, R.J.; Argo, M.K.; Dullo, B.T.; Knapen, J.H.; Brinks, E.; Muxlow, T.W.B.; Aalto, S.; et al. LeMMINGS—I. The eMERLIN legacy survey of nearby galaxies. 1.5-GHz parsec-scale radio structures and cores. *Mon. Not. R. Astron. Soc.* **2018**, *476*, 3478–3522. [[CrossRef](#)]
124. Doi, A.; Asada, K.; Nagai, H. Very Long Baseline Array Imaging of Parsec-scale Jet Structures in Radio-loud Narrow-line Seyfert 1 Galaxies. *Astrophys. J.* **2011**, *738*, 126. [[CrossRef](#)]
125. Richards, J.L.; Lister, M.L. Kiloparsec-Scale Jets in Three Radio-Loud Narrow-Line Seyfert 1 Galaxies. *Astrophys. J.* **2015**, *800*, L8. [[CrossRef](#)]
126. Richards, J.L.; Lister, M.L.; Savolainen, T.; Homan, D.C.; Kadler, M.; Hovatta, T.; Readhead, A.C.S.; Arshakian, T.G.; Chavushyan, V. The parsec-scale structure, kinematics, and polarization of radio-loud narrow-line Seyfert 1 galaxies. In Proceedings of the Extragalactic Jets from Every Angle, Galapagos Islands, Ecuador, 15–19 September 2014; Massaro, F., Cheung, C.C., Lopez, E., Siemiginowska, A., Eds.; Cambridge University Press: Cambridge, UK, 2015; Volume 313, pp. 139–142. [[CrossRef](#)]
127. Neff, S.G.; de Bruyn, A.G. The compact radio core of MKN 348: Evidence for directed outflow in a type 2 Seyfert galaxy. *Astron. Astrophys.* **1983**, *128*, 318–324.
128. Blandford, R.D.; Königl, A. Relativistic jets as compact radio sources. *Astrophys. J.* **1979**, *232*, 34–48. [[CrossRef](#)]
129. Baczkó, A.K.; Schulz, R.; Kadler, M.; Ros, E.; Perucho, M.; Fromm, C.M.; Wilms, J. Asymmetric jet production in the active galactic nucleus of NGC 1052. *Astron. Astrophys.* **2019**, *623*, A27. [[CrossRef](#)]
130. Baczkó, A.K.; Ros, E.; Kadler, M.; Fromm, C.M.; Boccardi, B.; Perucho, M.; Krichbaum, T.P.; Burd, P.R.; Zensus, J.A. Ambilateral collimation study of the twin-jets in NGC 1052. *Astron. Astrophys.* **2022**, *658*, A119. [[CrossRef](#)]
131. Simpson, C.; Mulchaey, J.S.; Wilson, A.S.; Ward, M.J.; Alonso-Herrero, A. An Ionization Cone and Dusty Disk in Markarian 348: The Obscuring Torus Revealed? *Astrophys. J.* **1996**, *457*, L19. [[CrossRef](#)]
132. Mezger, P.G.; Henderson, A.P. Galactic H II Regions. I. Observations of Their Continuum Radiation at the Frequency 5 GHz. *Astrophys. J.* **1967**, *147*, 471. [[CrossRef](#)]
133. Kharb, P.; Vaddi, S.; Sebastian, B.; Subramanian, S.; Das, M.; Paragi, Z. A Curved 150 pc Long Jet in the Double-peaked Emission-line AGN KISSR 434. *Astrophys. J.* **2019**, *871*, 249. [[CrossRef](#)]
134. Ulvestad, J.S.; Wrobel, J.M.; Roy, A.L.; Wilson, A.S.; Falcke, H.; Krichbaum, T.P. Subrelativistic Radio Jets and Parsec-Scale Absorption in Two Seyfert Galaxies. *Astrophys. J.* **1999**, *517*, L81–L84. [[CrossRef](#)]
135. Alexander, T.; Sturm, E.; Lutz, D.; Sternberg, A.; Netzer, H.; Genzel, R. Infrared Spectroscopy of NGC 4151: Probing the Obscured Ionizing Active Galactic Nucleus Continuum. *Astrophys. J.* **1999**, *512*, 204–223. [[CrossRef](#)]
136. Clemens, M.S.; Scaife, A.; Vega, O.; Bressan, A. Starburst evolution: Free-free absorption in the radio spectra of luminous IRAS galaxies. *Mon. Not. R. Astron. Soc.* **2010**, *405*, 887–897. [[CrossRef](#)]
137. Walterbos, R.A.M.; Braun, R. Diffused ionized gas in the spiral galaxy M31. *Astrophys. J.* **1994**, *431*, 156–171. [[CrossRef](#)]
138. Baldi, R.D.; Williams, D.R.A.; McHardy, I.M.; Beswick, R.J.; Brinks, E.; Dullo, B.T.; Knapen, J.H.; Argo, M.K.; Aalto, S.; Alberdi, A.; et al. LeMMINGS—II. The eMERLIN legacy survey of nearby galaxies. The deepest radio view of the Palomar sample on parsec scale. *Mon. Not. R. Astron. Soc.* **2021**, *500*, 4749–4767. [[CrossRef](#)]
139. Kharb, P.; Subramanian, S.; Vaddi, S.; Das, M.; Paragi, Z. Double-peaked Emission Lines Due to a Radio Outflow in KISSR 1219. *Astrophys. J.* **2017**, *846*, 12. [[CrossRef](#)]

140. Nevin, R.; Comerford, J.; Müller-Sánchez, F.; Barrows, R.; Cooper, M. The Origin of Double-peaked Narrow Lines in Active Galactic Nuclei. II. Kinematic Classifications for the Population at  $z < 0.1$ . *Astrophys. J.* **2016**, *832*, 67. [[CrossRef](#)]
141. Nevin, R.; Comerford, J.M.; Müller-Sánchez, F.; Barrows, R.; Cooper, M.C. The origin of double-peaked narrow lines in active galactic nuclei—III. Feedback from biconical AGN outflows. *Mon. Not. R. Astron. Soc.* **2018**, *473*, 2160–2187. [[CrossRef](#)]
142. Allen, M.G.; Groves, B.A.; Dopita, M.A.; Sutherland, R.S.; Kewley, L.J. The MAPPINGS III Library of Fast Radiative Shock Models. *Astrophys. J. Suppl. Ser.* **2008**, *178*, 20–55. [[CrossRef](#)]
143. Schmitt, H.R.; Donley, J.L.; Antonucci, R.R.J.; Hutchings, J.B.; Kinney, A.L. A Hubble Space Telescope Survey of Extended [O III]  $\lambda 5007$  Emission in a Far-Infrared Selected Sample of Seyfert Galaxies: Observations. *Astrophys. J. Suppl. Ser.* **2003**, *148*, 327–352. [[CrossRef](#)]
144. Schmitt, H.R.; Donley, J.L.; Antonucci, R.R.J.; Hutchings, J.B.; Kinney, A.L.; Pringle, J.E. A Hubble Space Telescope Survey of Extended [O III]  $\lambda 5007$  Å Emission in a Far-Infrared-Selected Sample of Seyfert Galaxies: Results. *Astrophys. J.* **2003**, *597*, 768–779. [[CrossRef](#)]

**Disclaimer/Publisher's Note:** The statements, opinions and data contained in all publications are solely those of the individual author(s) and contributor(s) and not of MDPI and/or the editor(s). MDPI and/or the editor(s) disclaim responsibility for any injury to people or property resulting from any ideas, methods, instructions or products referred to in the content.